

Observation and measurements of vector-boson scattering with the ATLAS experiment

Philip Sommer* on behalf of the ATLAS Collaboration

The University of Sheffield

E-mail: philip.sommer@cern.ch

The scattering of electroweak gauge bosons tests the gauge structure of the Standard Model and is sensitive to anomalous quartic gauge couplings. In this talk, recent results on vector-boson scattering from the ATLAS experiment using proton–proton collisions at $\sqrt{s} = 13$ TeV are presented. These include the observation of WZ and same-sign WW production via vector-boson scattering along with studies of VV production in semileptonic final states. Measurements of ZZ production via vector-boson scattering are also presented. The measured cross sections are compared to theoretical predictions. The sensitivity of these predictions to the choices of renormalisation and factorisation scales, the Parton Distribution Functions and showering models is studied in detail for the case of electroweak scattering of two same-sign W bosons in association with two jets and a number of event generator configurations are compared.

*European Physical Society Conference on High Energy Physics - EPS-HEP2019 -
10-17 July, 2019
Ghent, Belgium*

*Speaker.

1. Introduction

Vector boson scattering (VBS) is amongst the rarest processes currently accessible experimentally at the LHC. These processes occur, when in pp collisions two electroweak gauge bosons are produced in association with two jets and subsequently interact through trilinear and quartic gauge-boson self couplings, or through the exchange of a Higgs boson. Processes involving VBS diagrams can be used to study electroweak symmetry breaking which ensures the renormalisability of these interactions in the Standard Model. The ATLAS experiment [1] has studied VBS by measuring the electroweak production of $W^\pm W^\pm$ and WZ bosons, with the W and Z bosons decaying to leptons, as well as the electroweak production of VV ($V = W, Z$) bosons, with one gauge boson decaying to leptons and the other decaying hadronically. Data corresponding to 36.1 fb^{-1} of pp collision at $\sqrt{s} = 13 \text{ TeV}$ were used. More recently, the electroweak production of ZZ bosons with each Z boson decaying to a lepton pair has been studied using 139 fb^{-1} of pp collisions.

At the LHC, two gauge bosons in association with two jets can be produced at Born level in purely electroweak interactions or in mixed strong and electroweak interactions. Only the purely electroweak production involves VBS diagrams. Since no colour is exchanged between the incoming partons, the electroweak production can be separated from the strong production by its characteristic signature of two high p_T jets in the forward region with a large separation in rapidity. When reporting results for the electroweak production, interference effects between electroweak and strong production are typically assigned as a systematic uncertainty in the signal, therefore introducing a dependence of the measurement on theoretical predictions. This dependence is reduced when reporting the combined cross section of electroweak and strong production as a result.

2. Observation of electroweak $W^\pm W^\pm jj$ production

The $W^\pm W^\pm jj$ final state has the largest ratio of electroweak and strong production processes since gluon initiated diagrams are heavily suppressed. Purely electroweak diagrams without gauge-boson self interactions are suppressed as well. It is, hence, ideally suited for VBS studies. Candidate events are selected by requiring exactly two leptons, $\ell = e$ or μ , with the same electric charge, missing transverse momentum induced by the neutrinos, and at least two jets [2] with a rapidity separation. The signal is extracted in a fit of simulated signal events and the estimated background yields to five bins of the dijet invariant mass distribution, separately for ee , $e\mu$ and $\mu\mu$ final states and with positive and negative electric charge. The background from $WZjj$ production is constrained in a control sample selected with exactly three leptons and a normalisation factor of 0.86 ± 0.07 (stat.) $^{+0.18}_{-0.08}$ (exp. syst.) $^{+0.31}_{-0.23}$ (mod. syst.) is obtained.

The selected $W^\pm W^\pm jj$ candidate events show an excess of events with respect to the background-only hypothesis which is rejected with 6.5σ . The excess is consistent with the electroweak $W^\pm W^\pm jj$ signal for which a fiducial cross section of:

$$\sigma_{W^\pm W^\pm jj\text{-EW}}^{\text{fid.}} = 2.89_{-0.48}^{+0.51} \text{ (stat.)}_{-0.22}^{+0.24} \text{ (exp. syst.)}_{-0.16}^{+0.14} \text{ (mod. syst.)}_{-0.06}^{+0.08} \text{ (lumi.) fb}$$

is measured. The corresponding cross sections predicted by the Sherpa 2.2.2 [3] and PowhegBox+Pythia8 [4] event generators are $2.01_{-0.23}^{+0.33} \text{ fb}$ and $3.08_{-0.46}^{+0.48} \text{ fb}$, respectively. The

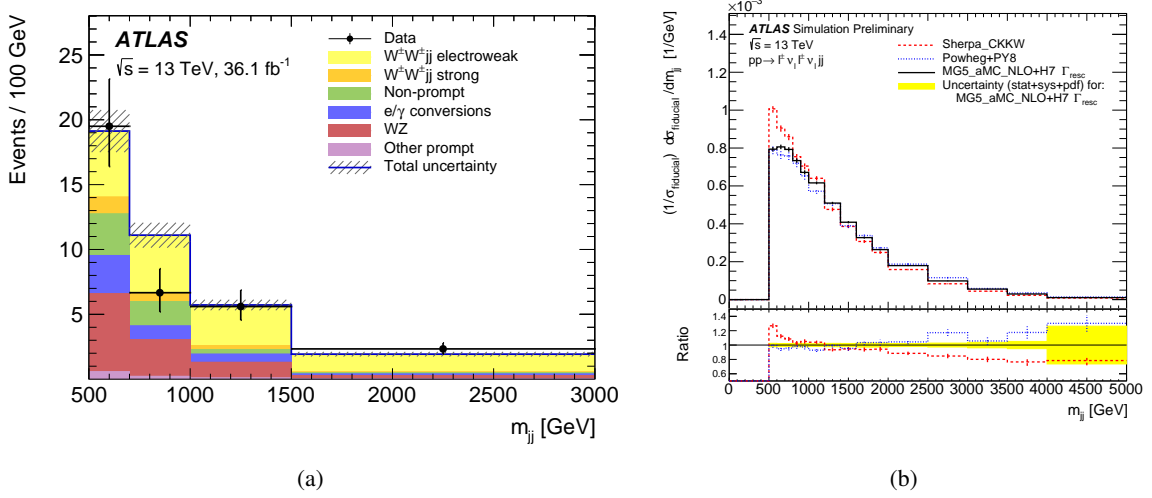


Figure 1: Distributions of the dijet invariant mass for electroweak $W^\pm W^\pm jj$ production. (a) The candidate events selected in data are shown with the estimated signal and background contributions. Systematic uncertainties are shown as a hatched band. The signal has been simulated with Sherpa 2.2.2 [2]. (b) The differential fiducial cross sections normalised to unity are shown for various event generators. Due to a non-optimal colour flow setting in Sherpa the total cross section significantly differs from that of Powheg or MG5_aMC@NLO. The effects on the normalised dijet invariant mass distribution are only up to 20% [5].

dijet invariant mass distribution of the selected candidate events, summed over all final states, is shown in Figure 1a.

Whilst the prediction from PowhegBox+Pythia8 agrees well with the measurement, the prediction from Sherpa 2.2.2 is approximately 30% lower. This can be explained by a non-optimal colour-flow setting for the parton shower in Sherpa 2.2.2 in VBS diagrams which leads to an excess of central jet emissions. Since for $W^\pm W^\pm jj$ production a multi-leg configuration is used these effects are partially mitigated. This, however, causes a significant underestimation of the total cross section. Comparisons of theoretical predictions with various configurations of event generators and parton-shower programs show that Sherpa 2.2.2 differs by up to 40% in the tails of the dijet invariant mass distribution [5], as shown in Figure 1b. Using the bin boundaries of the analyses, the differences are of the same size or smaller than the statistical uncertainties in the data. Within the modelling uncertainties derived using the dependence of the Sherpa 2.2.2 prediction on renormalisation and factorisation scales, different PDF sets, and variations of the matching and resummation scales in the combination of the matrix element with the parton shower, no significant effect was found in the measured cross section.

3. Observation of electroweak $WZjj$ production

A measurement of the combined strong and electroweak production is performed in a fiducial phase space enriched in events from electroweak $WZjj$ production [6]. Three leptons, two of

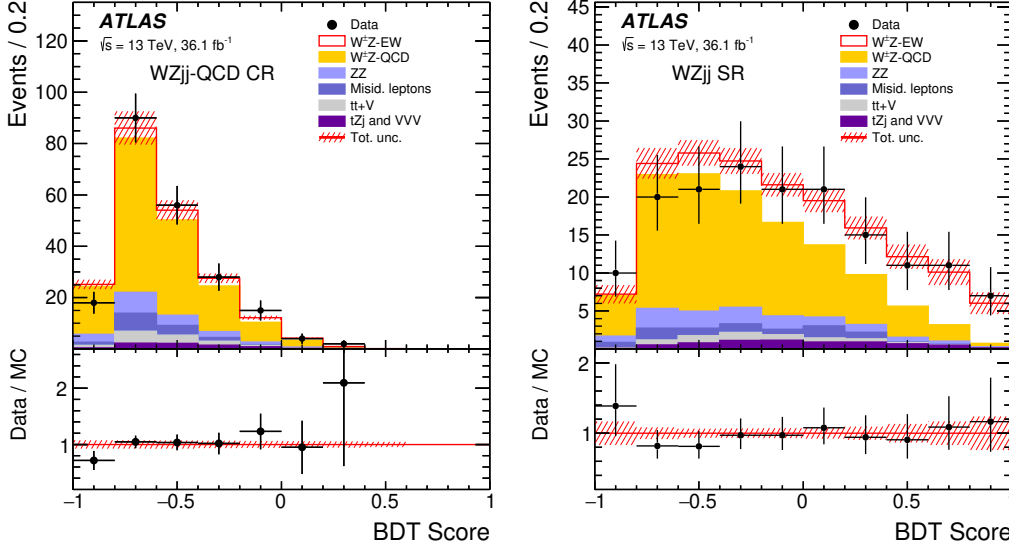


Figure 2: Distributions of the BDT discriminant used to extract the signal in the measurement of electroweak $WZjj$ production. The BDT is optimised using fifteen kinematic variables. The distribution is shown in a phase space dominated by strong $WZjj$ production (left) and in the fiducial phase space region (right). The events selected in data are shown with the estimated signal and background contributions. Systematic uncertainties are shown as a hatched band [6].

which have the same flavour, opposite electric charge, and an invariant mass consistent with a Z boson, and the other forms a transverse mass consistent with a W boson together with the neutrino, and two jets are required. Additional kinematic regions are used to constrain the background from $ZZjj$ and $t\bar{t}V$ production, and the strong production process. As in the measurement of $W^\pm W^\pm jj$ production, a significant overestimation of the strong $WZjj$ production by simulation is observed and a normalisation factor of 0.56 ± 0.16 is obtained in the fit. The combined electroweak and strong $WZjj$ production cross section is measured to be:

$$\sigma_{WZjj\text{-QCD+EW}}^{\text{fid.}} = 1.68 \pm 0.16 \text{ (stat.)} \pm 0.12 \text{ (exp. syst.)} \pm 0.13 \text{ (mod. syst.)} \pm 0.04 \text{ (lumi.) fb}$$

and differential cross sections are measured in several variables.

The ratio of strong and electroweak production is predicted to be much larger in $WZjj$ than in $W^\pm W^\pm jj$ production. To separate the strong and electroweak production, a BDT discriminant is optimised using fifteen variables related to the kinematics of the jets, the diboson system and combined jet–diboson variables. It is shown in Figure 2 in the region enriched in strong production and in the fiducial phase space. The simulation of the strong production is found to model the BDT discriminant well after the normalisation has been corrected. The electroweak signal is extracted in a fit to the BDT discriminant and the background-only hypothesis is rejected with 5.3σ where 3.2σ are expected. The excess corresponds to a fiducial electroweak $WZjj$ cross section of:

$$\sigma_{WZjj\text{-EW}}^{\text{fid.}} = 0.57_{-0.13}^{+0.14} \text{ (stat.)}_{-0.04}^{+0.05} \text{ (exp. syst.)}_{-0.04}^{+0.05} \text{ (mod. syst.)} \pm 0.01 \text{ (lumi.) fb}$$

compared to $0.321_{-0.024}^{+0.028}$ fb predicted by Sherpa 2.2.2.

Since the simulation of the electroweak signal process does not include additional partons in the matrix element, the analysis is more sensitive to the effects of the colour flow configuration in `Sherpa 2.2.2`. The difference of the BDT distribution simulated with `Sherpa 2.2.2` and `MG5_aMC@NLO` [7] is therefore included as a systematic uncertainty of the modelling of the simulated signal events in the measured cross section.

4. Search for electroweak diboson production in semileptonic decays

Compared to measurements of VBS processes where the gauge bosons decay to leptons, higher event yields can be reached if one of the gauge bosons can decay to hadrons. A study of these processes has been conducted, where a leptonically decaying gauge boson is reconstructed from two neutrinos ($Z \rightarrow \nu\nu$), one charged lepton and one neutrino ($W \rightarrow \ell\nu$), or two charged leptons ($Z \rightarrow \ell\ell$) [8]. A hadronically gauge boson is reconstructed from either one jet reconstructed with the anti- k_r algorithm and radius parameter $R = 1.0$, or two jets reconstructed with radius parameter $R = 0.4$. Jets reconstructed with $R = 1.0$ are further classified into high- and low-purity candidates using jet substructure variables. If no such jet can be found, two $R = 0.4$ jets are selected instead. In addition, two high- p_T jets reconstructed with $R = 0.4$ produced in association with the VV system are required in all categories.

The largest source of background in these events is V +jets production where a single gauge-boson is produced in association with jets from initial state radiation, followed by top quark production. The V +jets background contributions are constrained in dedicated kinematic regions, one for each of the nine signal regions. Background from top quark production can be significant for 1-lepton final states where dedicated control samples are defined for this background. The data events observed in every signal category and every control sample are shown in Figure 3a with the estimated background contributions. Respectively 0.5%, 1% and 3% of the selected data are expected to originate from electroweak $VVjj$ production if two $R = 0.4$ jets, a low-purity $R = 1.0$ jet or a high-purity $R = 1.0$ jet are selected.

The signal is extracted in a fit to BDT discriminants where a separate BDT is optimised for every combination of lepton final state, and jets reconstructed with $R = 1.0$ and $R = 0.4$. In total, distributions in 21 different kinematic regions are combined in the fit. The resulting data, signal and background yields are shown as a function of the signal-to-background ratio obtained in each bin of the fit in Figure 3b. The background-only hypothesis is rejected with 2.7σ where 2.5σ are expected from the theoretical prediction from `MG5_aMC@NLO`. A cross section of:

$$\sigma_{VVjj\text{-EW}}^{\text{fid.}} = 45.1 \pm 8.6 \text{ (stat.)}_{-14.6}^{+15.9} \text{ (syst.) fb}$$

is measured in the combined fiducial phase space region, in agreement with 43.0 ± 2.4 fb predicted by theory. Fiducial cross sections are also reported for each final state individually. The large systematic uncertainties are mainly related to the estimation of the V +jets backgrounds. There is the possibility to improve these uncertainties in future measurements on a larger dataset.

5. Search for electroweak $ZZjj$ production

Electroweak $ZZjj$ production was studied with the ZZ system decaying to 4ℓ and $2\ell 2\nu$ final states. Cross sections are measured for the combined strong and electroweak $ZZjj$ production in a

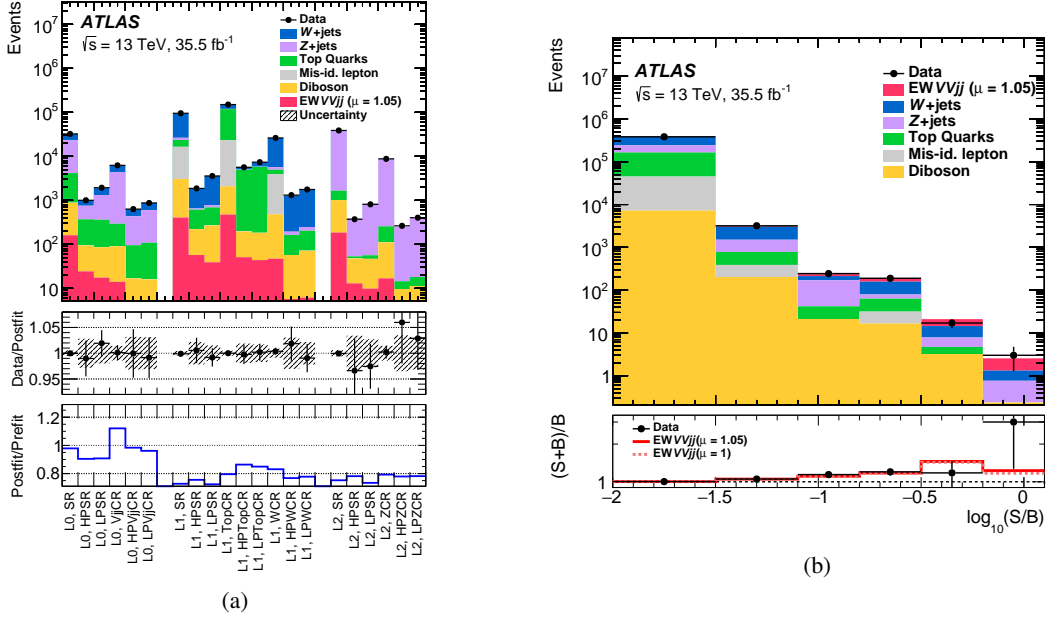


Figure 3: (a) Event yields of the selected data are shown with the estimated contributions from background and the electroweak $VVjj$ signal in 21 kinematic phase space regions used in the analyses. The lower pads show the ratio of the yield in data and the sum of the estimated signal and background contributions, and the sum of the signal and background yields estimated in the fit and predicted from simulation. The x -axis labels L0, L1 and L2 indicate the number of leptons selected and whether the region is primarily defined to extract the signal (SR) or constrain the background (CR). (b) Event yields as a function of the signal-to-background ratio, S/B , obtained in the various bins used in the fit to extract the electroweak $VVjj$ signal. The distribution is shown for data with estimated signal and background contributions. Only statistical uncertainties are shown [8].

phase space enriched in electroweak events [9]. They are measured to be:

$$\begin{aligned}\sigma_{4\ell jj\text{-QCD+EW}}^{\text{fid.}} &= 1.27 \pm 0.12 \text{ (stat.)} \pm 0.08 \text{ (syst.) fb} \\ \sigma_{2\ell 2\nu jj\text{-QCD+EW}}^{\text{fid.}} &= 1.22 \pm 0.30 \text{ (stat.)} \pm 0.18 \text{ (syst.) fb}\end{aligned}$$

in agreement with the theoretical predictions from MG5_aMC@NLO of 1.14 ± 0.20 fb and 1.07 ± 0.12 fb, respectively.

The electroweak signal is extracted in a fit to a BDT discriminant optimised using 12 and 13 variables for 4ℓ and $2\ell 2\nu$ categories, respectively. The BDT discriminants are shown in Figure 4. Electroweak $ZZjj$ production is observed for the first time with the background-only hypothesis rejected with 5.5σ and 4.3σ expected from MG5_aMC@NLO. The cross section in the combined fiducial 4ℓ and $2\ell 2\nu$ phase space is measured to be:

$$\sigma_{ZZjj\text{-EW}}^{\text{fid.}} = 0.82 \pm 0.21 \text{ fb}$$

in agreement with the MG5_aMC@NLO prediction of 0.61 ± 0.03 fb.

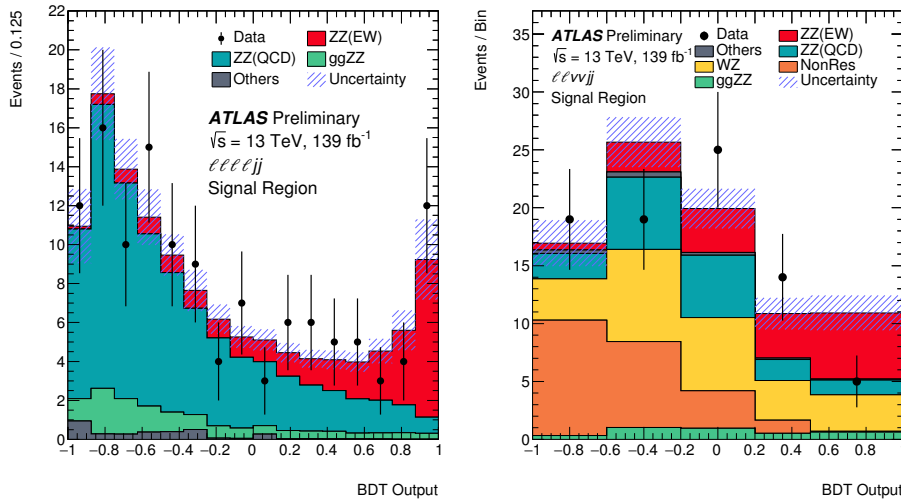


Figure 4: Distributions of the BDT discriminants used to extract the signal in the measurement of electroweak $ZZjj$ production. The events selected in data are shown with the estimated signal and background contributions. The distribution optimised for $lllljj$ final states (left) and $llvvjj$ final states are shown (right). Systematic uncertainties are shown as a hatched band [9].

6. Conclusions

In summary, recent studies of vector-boson scattering with the ATLAS experiment have been presented using pp collision data recorded in the years 2015 and 2016. In this dataset, the electroweak production of two electroweak gauge bosons in association with two jets was observed in the $W^\pm W^\pm jj$ and $WZjj$ final states. These are amongst the processes with the lowest cross section measured at the LHC to date. Subsequently, fiducial cross sections have been measured. Results for the combined strong and electroweak $WZjj$ production are presented in a phase space enriched in VBS events, including differential cross sections. Electroweak diboson production was also studied in the semileptonic decay mode and the background-only hypothesis was rejected with 2.7σ . The results presented use 36.1 fb^{-1} of the run-2 data recorded by ATLAS. Exploiting the full run-2 pp data amounting to 139 fb^{-1} allows for more detailed studies of vector-boson scattering, e.g. by making additional, more elusive final states, such as the electroweak $ZZjj$ production, experimentally accessible. The observation of this process was achieved in this dataset and reported for the first time in this presentation.

References

- [1] ATLAS Collaboration, JINST **3** (2008) S08003.
- [2] ATLAS Collaboration, arXiv:1906.03203 [hep-ex].
- [3] T. Gleisberg, S. Hoeche, F. Krauss, M. Schonherr, S. Schumann, F. Siegert and J. Winter, JHEP **0902** (2009) 007.
- [4] T. Melia, P. Nason, R. Rontsch and G. Zanderighi, Eur. Phys. J. C **71** (2011) 1670.
- [5] ATLAS Collaboration, ATL-PHYS-PUB-2019-004, <http://cds.cern.ch/record/2655303>.

- [6] ATLAS Collaboration, Phys. Lett. B **793** (2019) 469.
- [7] J. Alwall *et al.*, JHEP **1407** (2014) 079.
- [8] ATLAS Collaboration, Phys. Rev. D **100** (2019) no.3, 032007.
- [9] ATLAS Collaboration, ATLAS-CONF-2019-033, <https://cds.cern.ch/record/2682845>.